Immunophenotyping of Tumor-Infiltrating Immune Cells in Mouse Syngeneic Tumor Models Using Multi-Color Flow Cytometry Assays

The in vivo animal tumor models possessing fully functional immunity are essential for preclinical research of new immunotherapeutic medicine. Syngeneic tumor models are excellent in vivo animal models meeting the need for preclinical research and development of innovative immunotherapies as their homografts are developed from immortalized mouse tumor cell lines originated from the same inbred mouse strains with fully competent immunity. Therefore, syngeneic tumor models are ideal for assessing new single and combinational immunotherapies.

Immuno-oncological studies have shown that immune cell infiltration in the tumor microenvironment plays a critical role in cancer development and affects the clinical outcomes of cancer patients. Therefore, comprehensive profiling of tumor-infiltrating immune cells is important for delineating the mechanisms of cancer-immune evasion and propelling the development of novel immunotherapeutic strategies. For a deep understanding of the effects of immunotherapies on the immune ecosystem in the tumor, we need to use effective methods/strategies for immunoprofiling of the tumor microenvironment. Multi-color flow cytometry profiling of immune cell surface markers is one of the powerful, effective methods for elucidating the phenotypic profiles of immune cells infiltrating into the tumor microenvironment.

Noble Life Sciences (NLS) has GLP-compliance animal facilities for preclinical studies and provides various mouse syngeneic tumor models for preclinical research of new immunotherapeutic agents. NLS also has the in-house IVIS® Lumina In Vivo Imaging System for monitoring in vivo tumor growth during preclinical research of immuno-oncological therapies. Moreover, NLS has the flow cytometry facility for multi-color FACS analysis of immune cell type profiles in tumors and in tissues (e.g., bone marrow, spleen, etc.) with human hemopoietic stem cell engraftment, intracellular cytokine/protein expression of immune/cancer cells, cancer stem cell populations, etc. Other flow cytometry services include (but not limited to) apoptotic assays (e.g., Annexin V/7-AAD), cell cycle analysis, cell proliferation analysis (e.g., BrdU

incorporation assay), etc. NLS also offers custom-designed flow cytometry services by designing and validating FACS assays according to the client's need.

To demonstrate the multi-color flow cytometry service capability of Noble Life Sciences, we have established the flow cytometry assay workflow through the immunoprofiling study of tumor-infiltrating immune cells in two different syngeneic mouse tumor models (CT26 and 4T1) treated with the immune checkpoint inhibitor (anti-PD-1 monoclonal antibody) in comparison to their control counterparts.

Experimental Approaches

Step 1: Syngeneic tumor cell transplantation and animal dosing with anti-mouse PD-1 mAb.

Balb/c mice were transplanted with either CT26 (colorectal tumor) or 4T1 (breast tumor) cells (2 x 105 cells/mouse). Once their tumor sizes reached approximately 60 mm3, mice were treated with either vehicle (PBS) for the control group (n = 5) or anti-mouse PD-1 mAb (20 mg/kg) (Bio-X Cell Inc.) for the treatment group (n = 5) via intraperitoneal (IP) injection. Mice were dosed every 2 or 3 days five times before their euthanization for multi-color flow cytometry studies. The graphic diagram for the dosing scheme is shown below:

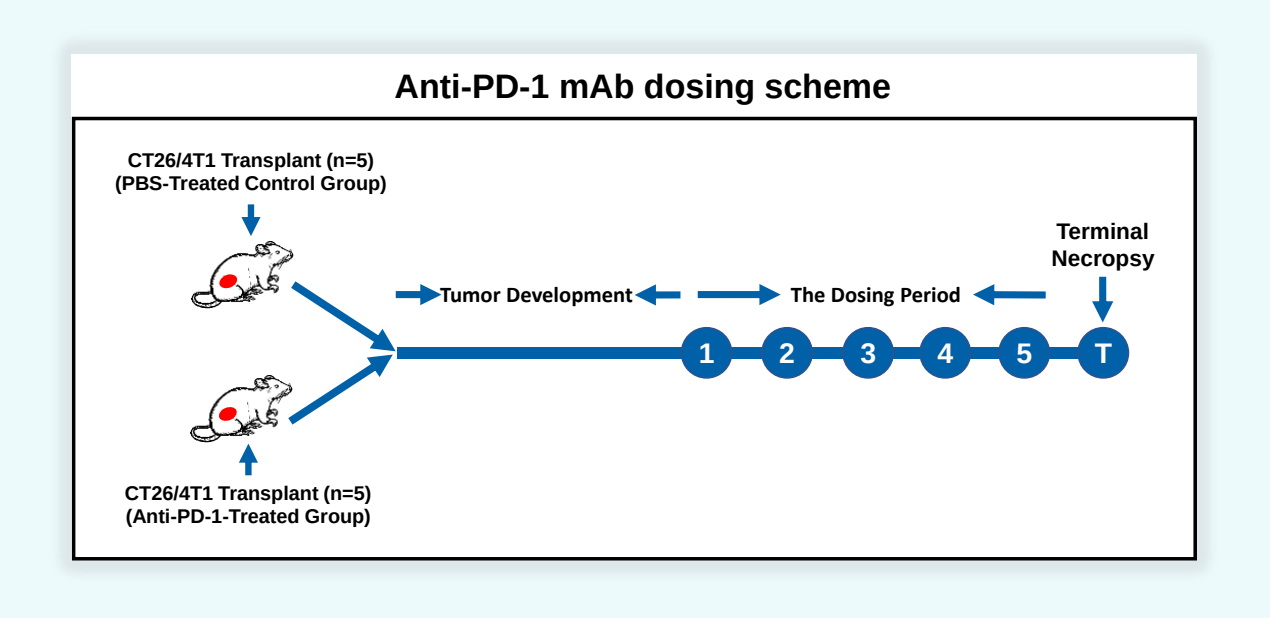

Step 2: Tumor tissue processing and tumor cell preparation.

Tumor tissue was processed using a gentleMACS™ Dissociator (Miltenyi Biotec) and single tumor cells were prepared using the Tumor Dissociation Kit for mouse (Miltenyi Biotec). This method has been optimized for the high yield of single tumor cells and tumor-infiltrating immune cells.

Step 3: Immunostaining of tumor-infiltrating immune cells.

Eight different fluorescence-conjugated antibodies were used to detect and quantify the lineage-specific surface markers for multiple tumor-infiltrating immune cell types. The antibodies used in the study and immune cell lineages detected by these Abs are listed below:

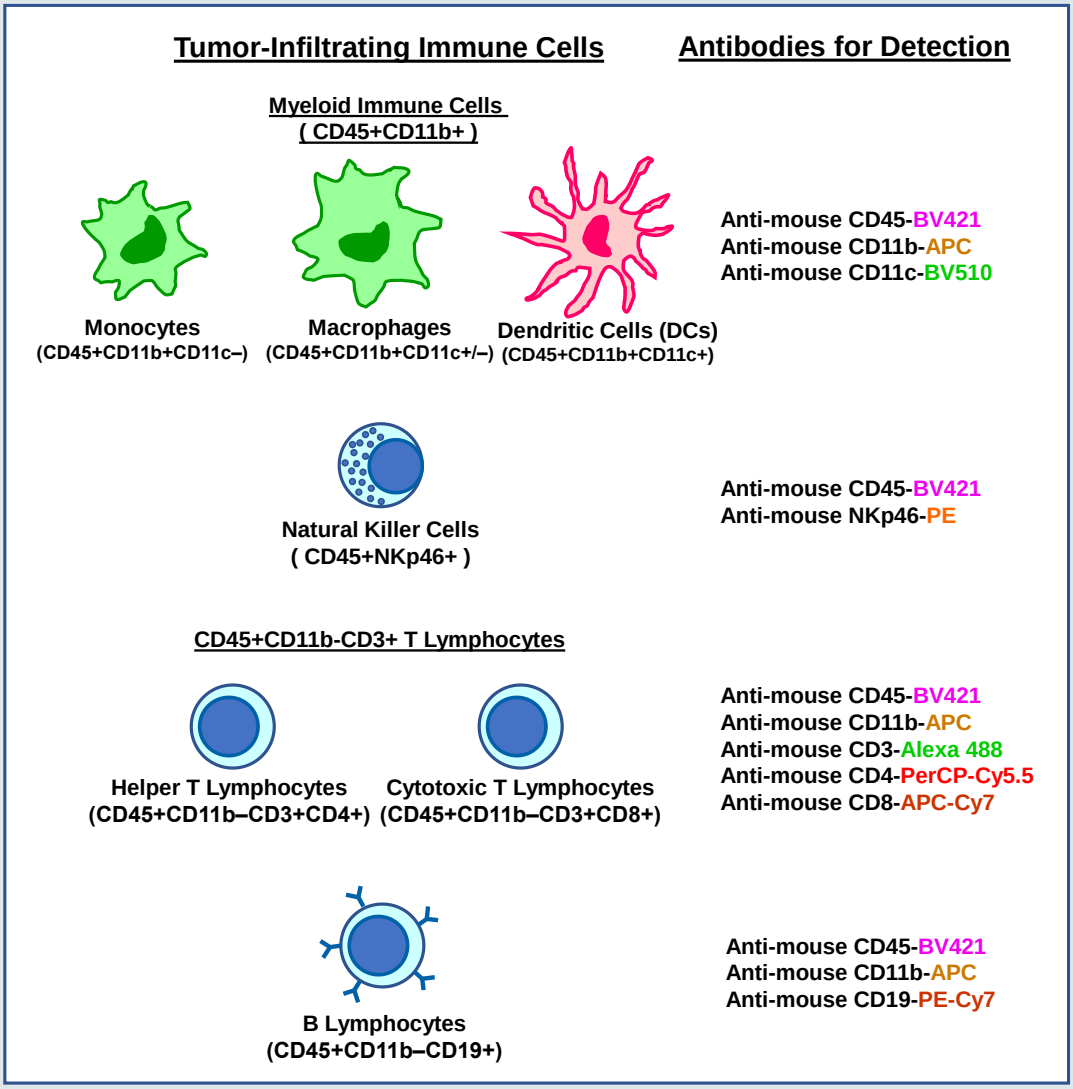

Step 4: Multi-color Flow Cytometry Assays.

The Miltenyi Biotec MACSQuant 10 Analyzer, a 3-laser 8-color system, was used for multi-color flow cytometry assays. The Raw flow data were analyzed using FlowJo software.

MACSQuant® 10 Analyzer
(3 lasers for detection of 8 fluorescent colors)

Results

The workflow design for flow cytometry data analysis of tumor-infiltrating immune cells.

To analyze the individual tumor-infiltrating immune cell types in CT26 and 4T1 syngeneic tumor models, NLS has developed the flow data analysis workflow as shown in Figures 1, 2 and 3.

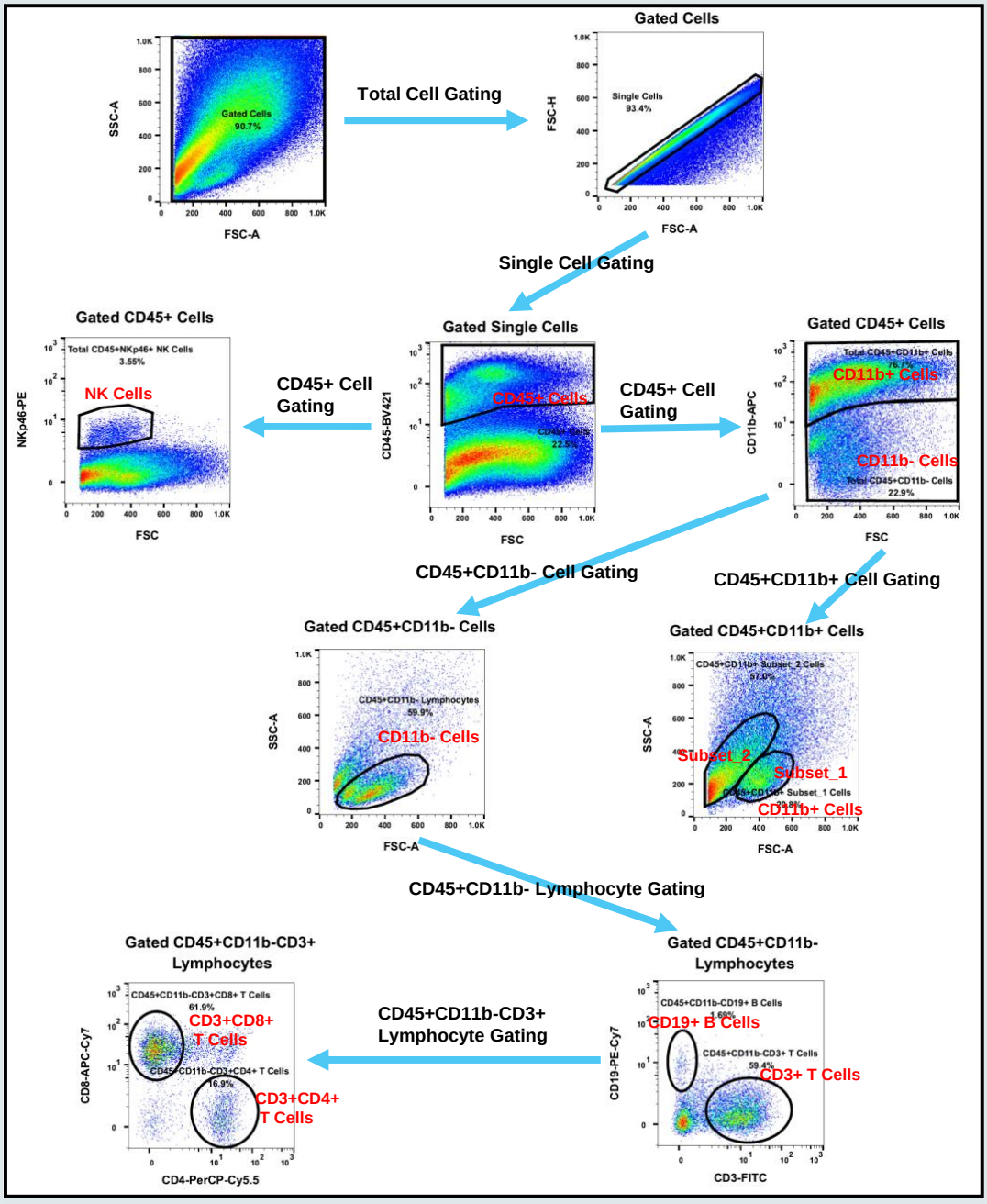

Figure 1. The workflow for flow cytometry data analysis of tumor-infiltrating immune cells in the CT26 tumor. There were two subsets of cell populations present in gated CD45+CD11b+ cells when they were displayed in a scatter plot of FSC-A vs SSC-A. The sizes of subset 1 cells were overall larger than subset 2 cells.

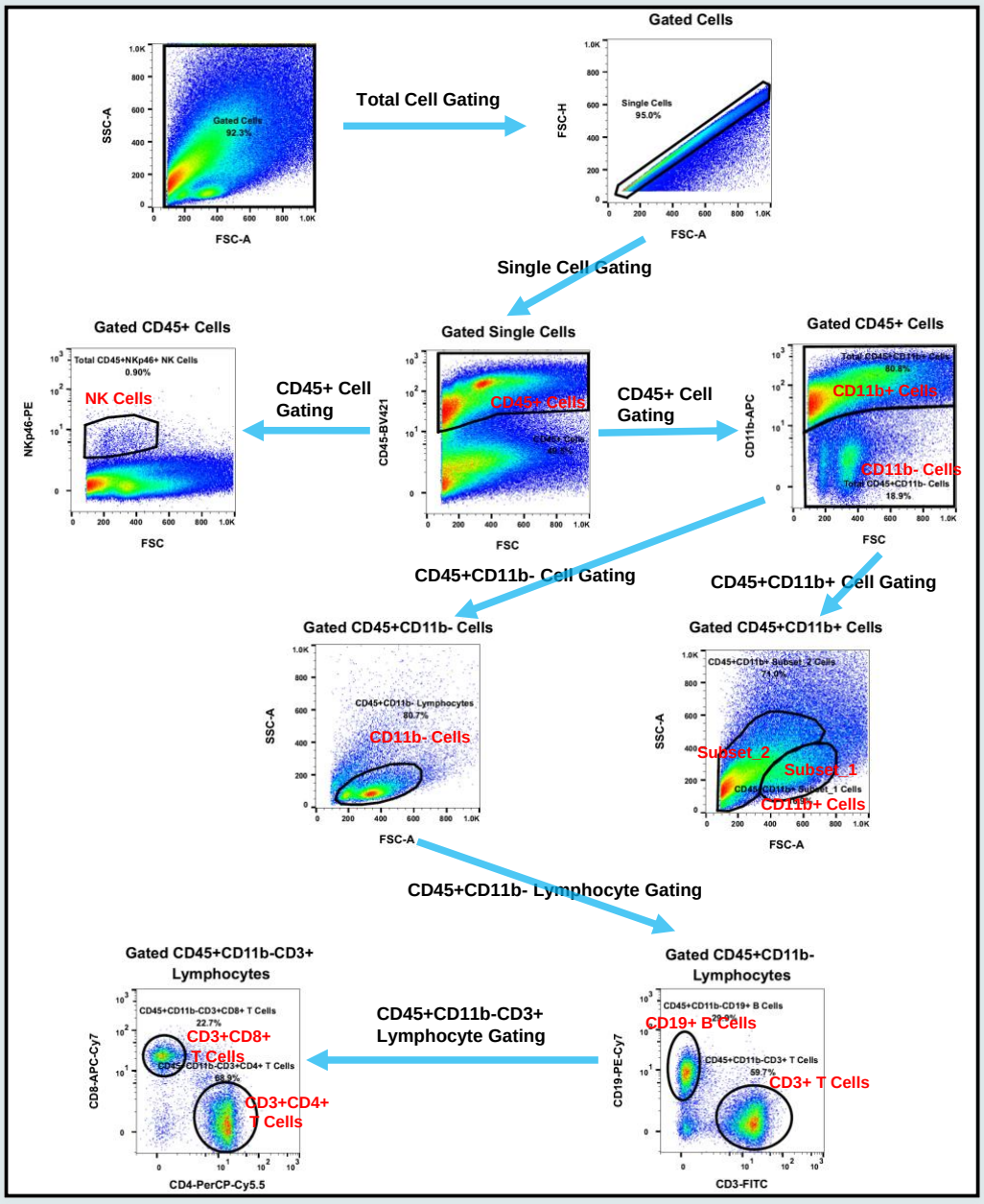

Figure 2. The workflow for flow cytometry data analysis of tumor-infiltrating immune cells in the 4T1 tumor. The same flow data analysis workflow shown in Figure 1 was applied to immunoprofiling of the 4T1 tumor.

Immunophenotyping of CT26 and 4T1 tumors showed that these two syngeneic colorectal and mammary gland tumor models displayed different profiles in their tumor-infiltrating immune ecosystems. For example, the predominant tumor-infiltrating lymphocytes (TILs) in CT26 tumors were CD3+CD8+ cytotoxic T cells (Figure 1), whereas CD3+CD4+ helper T cells were predominant TILs in 4T1 tumors (Figure 2). The majority of tumor-infiltrating CD45+ immune cells in both syngeneic tumor models

were CD11b+ myeloid cells (Figures 1 and 2), ranging from 60% to 95% of total CD45+ cells. Moreover, two subsets of cell populations were found to be present in a scatter plot of FSC-A vs SSC-A for gated CD45+CD11b+ cells (Figures 1 and 2). CD45+CD11b+ subset 1 cells expressed higher levels of CD11b than subset 2 cells and were mainly CD11c-positive, in contrast to subset 2 cells that were mainly CD11c-negative (Figure 3). Based on marker stratifications, CD45+CD11b+ subset 1 cells were mainly macrophages and dendritic cells (DCs) as judged from their larger cell sizes and positivity of CD11c (Figure 3). In contrast, CD45+CD11b+ subset 2 cells were mainly monocytes as judged from their smaller cell sizes and negativity of CD11c (Figure 3).

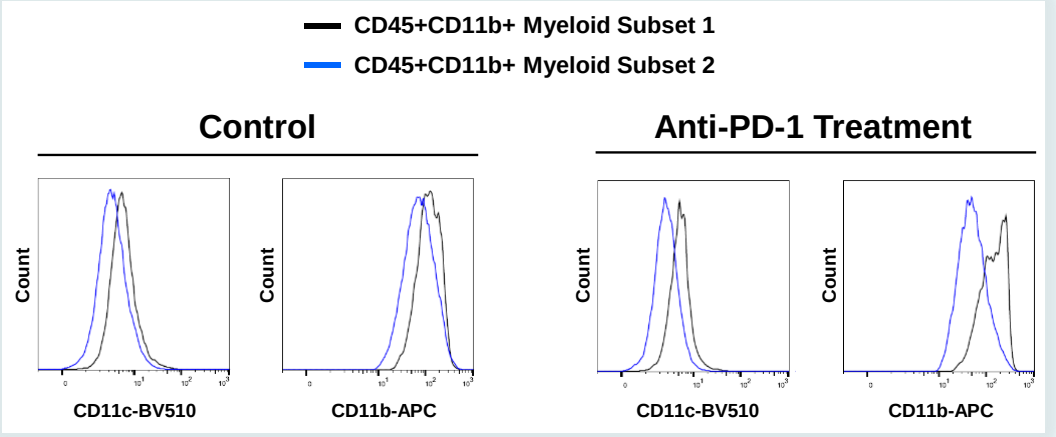

Figure 3. The stratification of CD45+CD11b+ myeloid cells using the CD11c marker. Subset 1 and subset 2 of CD45+CD11b+ myeloid cells shown in Figure 1 were further stratified by their expression of CD11b and CD11c (the dendritic cell marker). Stained tumor cell samples from control and treatment groups were analyzed.

Flow cytometric immunophenotyping of tumor-filtrating immune cells in CT26 syngeneic colorectal tumors treated with or without anti-mouse PD-1 mAb.

We employed the developed flow-cytometry-based methodology to delineate the effect of treatment with anti-mouse PD-1 mAb on syngeneic CT26 colorectal tumors. The tumor cell samples were prepared from collected tumor tissue samples, and then stained with fluorescence-conjugated antibodies specific to different immune cell lineages as described in experimental approaches. After the completion of antibody incubation and cell wash, stained tumor cell samples were analyzed by the MACSQuant 10 analyzer. Percentages of individual immune cell types in gated CD45+ cells were determined from analysis of the flow raw data using the analysis workflow shown in Figure 1.

As shown in Figure 4, there was no significant difference in total CD45+ cells between control and treated animal groups. However, anti-PD-1 mAb treatment had differential

effects on distinct immune cell lineages within CT26 tumors. The analyzed flow data showed that anti-PD-1 mAb treatment led to statistically significant decreases in tumor-infiltrating CD45+CD11b+ subset 1 myeloid cells ($p < 0.05$) that were mainly macrophages and dendritic cells (DCs) (Figure 4). Oppositely, anti-PD-1 mAb caused statistically significant increases in tumor-infiltrating CD45+CD11b+ subset 2 myeloid cells ($p < 0.05$) that were mainly monocytes (Figure 4). Moreover, anti-PD-1 mAb treatment tended to decrease tumor-infiltrating CD45+CD11b-CD3+ T cells ($p = 0.1098$), in particular CD45+CD11b-CD3+CD8+ cytotoxic T cells ($p = 0.0681$) (Figure 4).

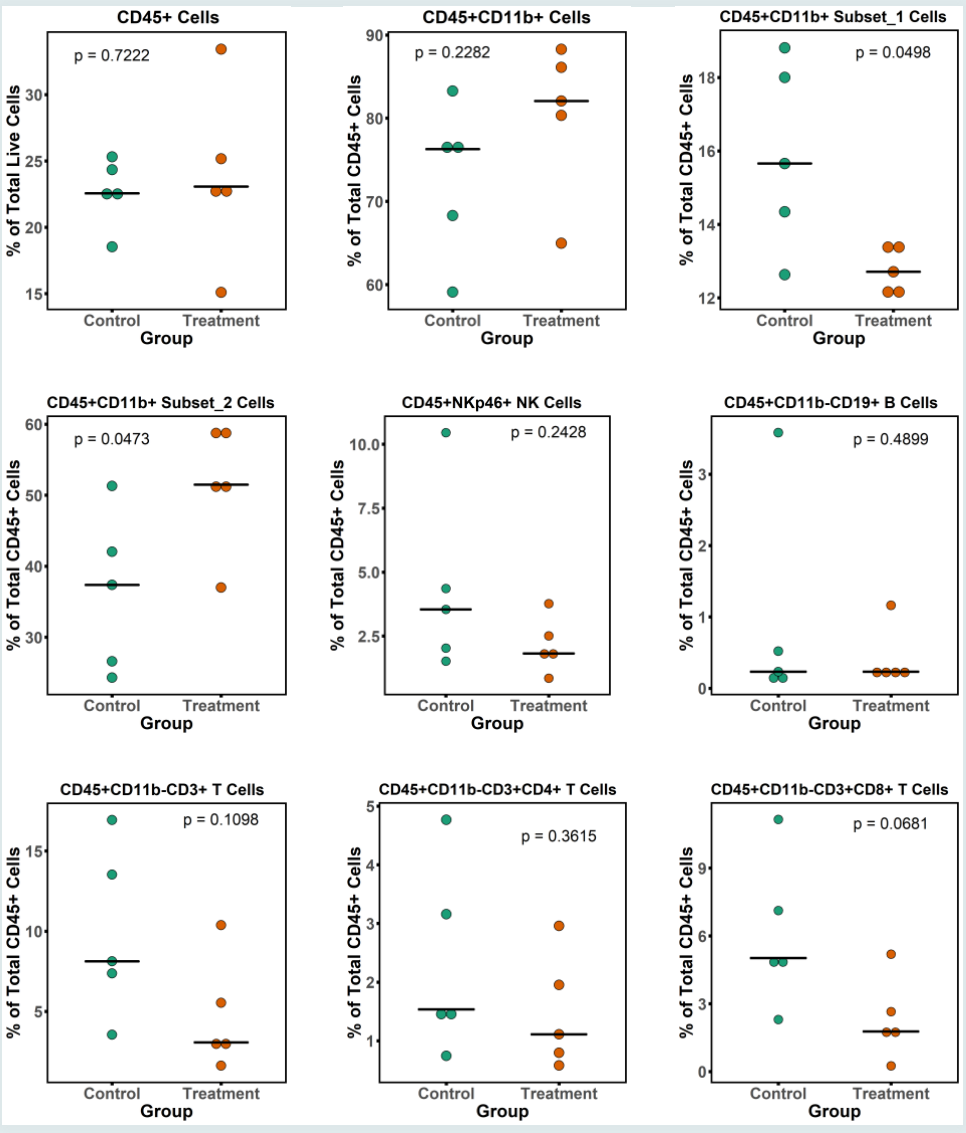

Figure 4. Multi-color flow cytometric analysis of infiltrated immune cells in CT26 syngeneic tumors with or without anti-PD-1 treatment. Except for CD45+ cells that were expressed as the percentage of total live cells, all other immune cell types were expressed as the percentages of total CD45+ cells. Statistical analyses for *p* values used the two-tailed Student's T-Test. The median of each data group is indicated by a horizontal bar.

Flow cytometric immunophenotyping of tumor-filtrating immune cells in 4T1 syngeneic mammary gland tumors treated with or without anti-mouse PD-1 mAb.

Tumor-infiltrating immune cell profiling of 4T1 tumors with or without treatment with anti-PD-1 mAb was analyzed and shown in Figure 5.

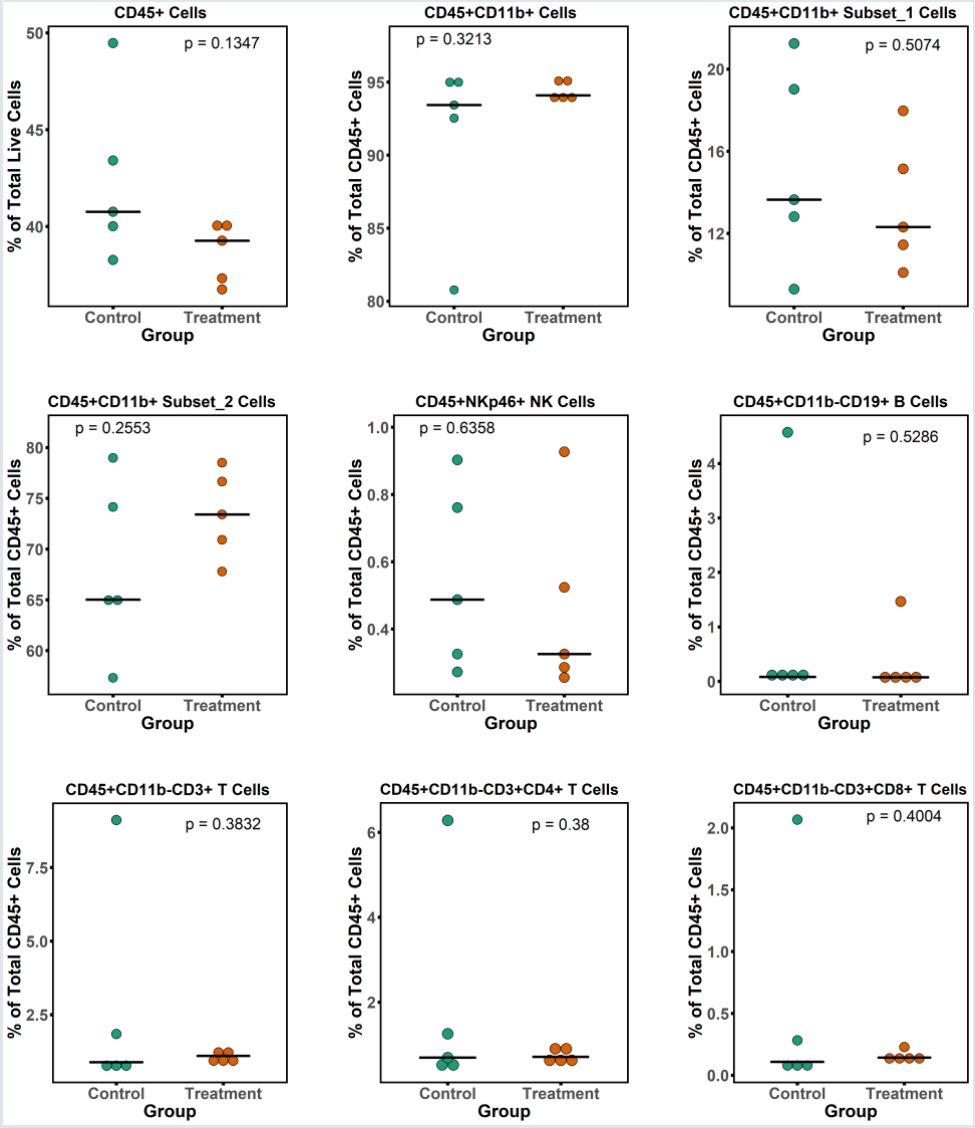

Figure 5. Multi-color flow cytometric analysis of infiltrated immune cells in 4T1 syngeneic tumors with or without anti-PD-1 treatment. Except for CD45+ cells that were expressed as the percentage of total live cells, all other immune cell types were expressed as the percentages of total CD45+ cells. Statistical analyses for *p* values used the two-tailed Student's T-Test. The median of each data group is indicated by a horizontal bar.

As shown in Figure 5, although treatment with anti-PD-1 mAb had no statistically significant effects on percentages of various immune cell lineages in gated CD45+ cells, there was a tendency that anti-PD-1 mAb treatment led to an increase in CD45+CD11b+ subset 2 myeloid cells ($p = 0.2553$), which was consistent with the CT26 flow data (Figure 4). Moreover, anti-PD-1 mAb seemed to decrease overall CD45+ cells in tumors ($p = 0.1347$) (Figure 5).

Conclusion

Through this study, we have established the procedures for preparing single tissue cells from dissected tumors and the multi-color flow cytometry assay workflow (up to 8 colors) for immunophenotyping of tumor-infiltrating immune cells and other applications. Our findings from this R&D study showed that tumor-infiltrating lymphocytes (T and Natural Killer cells) were found more in CT26 syngeneic tumors than in 4T1 syngeneic tumors. From the immune checkpoint inhibitor treatment study, we found that the percentages of tumor-infiltrating immune cells (e.g., T lymphocytes and myeloid cells) within CT26 tumors more responded to and were more significantly altered by treatment with anti-PD-1 mAb when compared to those within 4T1 tumors.

Moreover, CD45+CD11b+ subset 1 myeloid cells, mainly being macrophages and DCs, within CT26 tumors were significantly reduced by anti-PD-1 mAb treatment in a statistically meaningful manner. In contrast, anti-PD-1 mAb oppositely increased CD45+CD11b+ subset 2 myeloid cells, mainly being monocytes, within CT26 tumors. These findings suggest that the tumor-suppressive effect of anti-PD-1 mAb might have been through reducing transformed, tumor-promoting macrophages and DCs within tumors and enhancing the recruitment of peripheral tumor-suppressive monocytes to the tumor site. Given that there are complicated tumor-infiltrating immune cell lineages (e.g., CD14+ and CD16+ subsets of monocytes, M1/M2 macrophages, classic/plasmacytoid DCs, T cell subsets of CD4+, CD8+, TH1, TH2, TH17, and Tregs, etc.) can be explored, further studies using more immune-lineage-specific markers will be needed to reveal how anti-PD-1 mAb affects the tumor-infiltrating immune ecosystem.